Anomalously small $4f$-$5d$ oscillator strengths and $4f$-$4f$ electronic Raman scattering cross sections for Ce^{3+} in crystals of $LuPO_4$

G. M. Williams* and N. Edelstein
Department of Physics, University of California, Berkeley, California 94720
and Materials and Chemical Sciences Division, Lawrence Berkeley Laboratory, 1 Cyclotron Road, Berkeley, California 94720

L. A. Boatner and M. M. Abraham
Solid State Division, Oak Ridge National Laboratory, P.O. Box 2008, Oak Ridge, Tennessee 37831-6032
(Received 16 January 1989)

The oscillator strengths for the $4f^1 \rightarrow 5d^1$ transitions of Ce^{3+} in $LuPO_4$ were measured from absorption spectra and compared to calculated values. The measured oscillator strengths were found to be between 2.5 and 20 times smaller than the corresponding theoretical values. In addition, absolute cross sections for electronic Raman scattering between the levels of the $4f^1$ configuration of Ce^{3+} in $LuPO_4$ were measured and found to be significantly smaller than those expected from theory. Both of these discrepancies may be explained by a reduction in the radial integral, $\langle 4f|r|5d\rangle$, for Ce^{3+} in the solid state. Absorption data obtained from the literature for the $4f^1 \rightarrow 5d^1$ transitions of Ce^{3+} in a number of host crystals were used to establish a correlation between the cerium-ion–ligand distance and the reduction in the $\langle 4f|r|5d\rangle$ integral. Effects on electronic Raman scattering cross sections for rare-earth ions in crystals are discussed.

I. INTRODUCTION

Transparent crystals containing trivalent rare-earth ions form a unique and interesting class of optical materials, and accordingly, a great deal of effort has been directed toward establishing a quantitative description of the intensities of optical processes in these crystals. The Judd-Ofelt theory[1,2] for the intensities of the formally parity-forbidden, one-photon transitions between states of the ground $4f^N$ configuration of the trivalent rare-earth ions has proven, in general, to be quite successful—with the most notable flaw being the unexpected hypersensitivity[3–5] of one of the parameters of the theory to changes in the crystalline environment about the rare-earth ion.

The similarities between the Judd-Ofelt one-photon theory and the calculation of the intensities of two-photon transitions between states of the $4f^N$ configuration of rare-earth ions, as developed by Axe,[6] have led to studies comparing the observed and calculated intensities for two-photon processes. These studies serve as a new test of the approximations common to both calculations. The two-photon experiments potentially serve as a more stringent and thus more revealing test as a result of the reduced number of parameters needed to describe the parity-allowed two-photon transitions. Comprehensive comparisons between the observed and calculated intensities have been carried out by Downer *et al.*[7–10] using two-photon absorption in crystals of Eu^{2+}:LaF_3 and Gd^{3+}:LaF_3 and by Becker *et al.*[11,12] using electronic Raman scattering in crystals of $ErPO_4$ and $TmPO_4$. The observed discrepancies between experiment and calculation have spurred a number of papers suggesting extensions to the standard second-order theory of two-photon processes.[13–18]

Recently, Judd[19] has derived a simple expression for the sum of oscillator strengths for transitions of the type $4f^N \rightarrow 4f^{N-1}5d$. Using this expression, oscillator strength sums were computed for $f \rightarrow d$ transitions in Ce^{3+}, Tb^{3+}, and Bk^{3+} and compared to the observed values for these ions in aqueous solution.[20,21] It was found that the calculated values exceeded the observed values of factors ranging from 2 to greater than 10. This result is relevant to the intra-$4f^N$ one- and two-photon transition intensities because the expressions describing these intensities contain matrix elements of the electric dipole operator between states of the $4f^N$ and $4f^{N-1}5d$ configurations. Thus, if the measured $4f^N \rightarrow 4f^{N-1}5d$ oscillator strengths are smaller than theoretically expected, this implies that the intensities of the intra-$4f^N$ one- and two-photon transitions also should be smaller than expected.

This idea can be readily tested by comparing the observed absolute two-photon cross sections to those calculated from theory. Many previous experiments have compared the absolute intra-$4f^N$ one-photon oscillator strengths to those computed using the Judd-Ofelt theory, but in these cases any reduction in the oscillator strengths would be observed in empirical parameters of the theory. To note any reduction, the values of the fitted parameters have to be compared to the values of the parameters expected from physical estimates of such quantities as the strength of the crystal field, radial overlap integrals between configurations, and the average energies of excited configurations. The parameters of the two-photon theory are easier to estimate because they do not include the strength of the crystal field. Quantities such

as the radial overlap integrals and excited configuration energies may be estimated from Hartree-Fock calculations.

In the two-photon work by Downer *et al.*[7–10] and Becker *et al.*,[11,12] all intensities were calculated to within a factor that was dependent on both the radial overlap integrals and the excited-configuration average energies common for all transitions. For both studies, the calculated values were compared to the experimentally observed relative intensities between different transitions—thus eliminating the necessity of the factor determining the overall scaling for the absolute cross sections.

The measurement of absolute two-photon cross sections is difficult in both electronic Raman scattering and two-photon absorption because of the problems in obtaining the efficiency of the light-collection system. Chase and Payne,[22] in a carefully executed experiment, however, have succeeded in measuring absolute two-photon absorption cross sections for the $^4I_{9/2} \rightarrow {}^4G_{7/2}$ transition in Nd^{3+}-doped crystals of $Y_3Al_5O_{12}$ [yttrium aluminum garnet (YAG)] and $LiYF_4$ [yttrium lithium fluorite (YLF)]. A comparison with the calculated values showed that, for the YAG crystal, the measured cross section was as expected, but for the YLF crystal the measured cross section was smaller than expected by approximately a factor of 10. The small value of the cross section for the YLF crystal is in accord with the reduced $4f \rightarrow 5d$ oscillator strengths noted by Judd.[19]

We have recently reported the results of a comparison between the observed and calculated relative electronic Raman scattering intensities for Ce^{3+} in single crystals of $LuPO_4$.[23] Ce^{3+}, with a ground-state configuration $[Xe]4f^1$, has one optically active electron. A primary motivation for the study of Ce^{3+} was the relatively low energy of the excited $5d^1$ configuration that permitted direct spectroscopic observation of these states, which serve as the primary virtual intermediate states in the electronic Raman process. Thus, data have been obtained on both the electronic Raman scattering intensities and the $4f \rightarrow 5d^1$ absorption spectra. In this paper we report a careful analysis of the absorption data and a calibration of the efficiency of the electronic Raman scattering light-collection system from which the absolute values have been obtained for both the electronic Raman scattering cross sections and the $4f^1 \rightarrow 5d^1$ oscillator strengths. These "linked" quantities can then be compared to their respective calculated values.

II. ELECTRONIC ENERGY LEVELS AND WAVE FUNCTIONS

The wave functions for the states of both the $4f^1$ and $5d^1$ configurations are needed in order to compute the expected values for the $4f \rightarrow 5d$ absorption and the $4f \rightarrow 4f$ electronic Raman scattering cross sections. The angular parts of the wave functions were obtained from a parametric analysis of the observed energy levels of both the $4f^1$ ground and $5d^1$ excited configurations.[23] The energy-level diagram of Ce^{3+}:$LuPO_4$ is shown in Fig. 1. The angular wave functions for each of the energy levels can be written as a sum of Russell-Saunders terms:

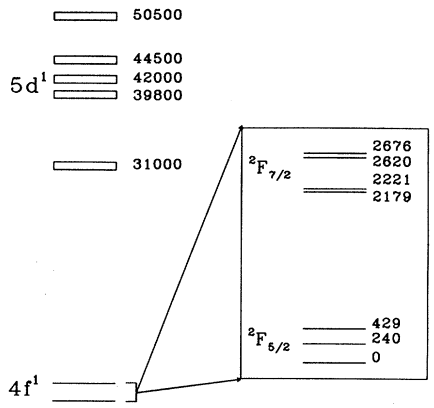

FIG. 1. Schematic representation of the energy-level structure of Ce^{3+} in a crystal of $LuPO_4$. Units are cm^{-1}.

$$|\Psi\rangle = \sum_{J,M_J} a_{J,M_J} |L,S,J,M_J\rangle \ . \tag{1}$$

The radial parts of the wave functions are also necessary for the calculation of absolute cross sections and have been calculated numerically with a relativistic Hartree-Fock code.[24] The radial integral $\langle 4f|r|5d\rangle$ has a value of 0.441 Å for the Ce^{3+} free ion.

III. $4f \rightarrow 5d$ ABSORPTION

A. Measurement of the oscillator strengths

Absorption spectra of Ce^{3+} in $LuPO_4$ were obtained in the range 29 000–51 000 cm^{-1} using a Cary 17 spectrophotometer purged with dry nitrogen gas. Throughout this paper, the absorption spectra are expressed in terms of α, as a function of wave number ($k = 1/\lambda$). The quantity α is given by the usual definition,

$$\alpha(k) = -\frac{1}{l} \ln \frac{I}{I_0} \ , \tag{2}$$

where I_0 and I are the intensities of the incident and transmitted light, respectively, and l is the crystal thickness. The oscillator strength P for a particular transition is proportional to the area under the spectral feature associated with the transition divided by the number density of absorbing ions n_0. This expression is

$$P = \left[\frac{1}{\pi r_0}\right] \frac{1}{n_0} \int_{\text{peak}} \alpha(k) dk \ , \tag{3}$$

where $r_0 = e^2/m_e c^2 \approx 2.813 \times 10^{-13}$ cm, and is the classical radius of the electron.

Crystals with three different doping levels of Ce^{3+} were studied. These crystals nominally has 1%, 10%, and 20% mode ratios of Ce to Lu in the starting materials used for crystal growth. In order to have a direct measure of the Ce^{3+} concentrations in the crystals, x-ray-fluorescence analyses[25] were utilized on the nominally 1% and 20% crystals. The analyses showed that the actual mole percent in the crystals was reduced greatly

from the starting proportions to values of 0.0604 and 0.638 mol %, respectively. The number density of Lu^{3+} in LuPO (Ref. 26) is 1.44×10^{22} cm^{-3}, so these concentrations correspond to Ce^{3+} number densities of 8.71×10^{18} and 9.19×10^{19} cm^{-3}. The relatively small values for the final Ce^{3+} concentrations are not surprising since the substitution of Ce^{3+} into Lu^{3+} sites is expected to be diminished as a result of the significantly larger ionic radius of Ce^{3+} compared to that of Lu^{3+}.[27]

The room-temperature absorption spectra for crystals with the three different concentrations of Ce^{3+} are shown in Fig. 2. The peaks labeled (a)–(d) and (f) have been previously identified[23] as $4f^1\rightarrow5d^1$ transitions of Ce^{3+}. This identification is confirmed by the observation that these peaks increase with increasing Ce^{3+} concentration. For the peak labeled (a) at 31 000 cm^{-1}, the integrated absorptions for the nominally 1% and 20% crystals scale approximately as 1 to 10, in agreement with the ratio of the concentrations determined from the x-ray-fluorescence analysis.

In Ce^{3+}:$LuPO_4$ it is expected that all absorption in the range 30 000–50 000 cm^{-1} will be solely due to the $4f^1\rightarrow5d^1$ transitions of the cerium ion. Pure $LuPO_4$ is transparent[28] to approximately 70 000 cm^{-1}, and transitions associated with charge transfer between the ligands and the cerium ions are expected to occur at a considerably higher energy than[29] 50 000 cm^{-1}. Reflection losses resulting from the refractive index of $LuPO_4$ are not expected to vary significantly with the excitation energy at energies so far removed from the band gap of $LuPO_4$. However, we observe in the spectra of Ce^{3+}:$LuPO_4$ absorption features which do not correlate with the cerium-ion concentration. These absorption features are in the form of several well-defined peaks in the 46 000–47 500-cm^{-1} range with a broad background over

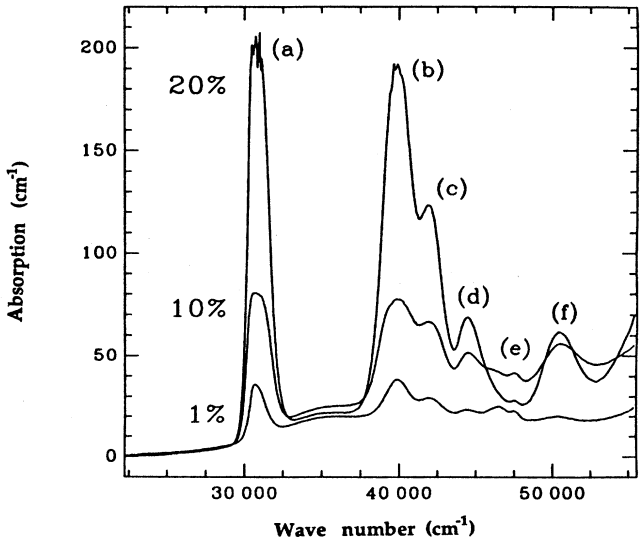

FIG. 2. Room-temperature absorption spectra of Ce^{3+}:$LuPO_4$ for three different concentrations of Ce^{3+}. Peaks (a)–(d) and (f) are attributed to absorption in cerium. Peak (e) is due to an impurity.

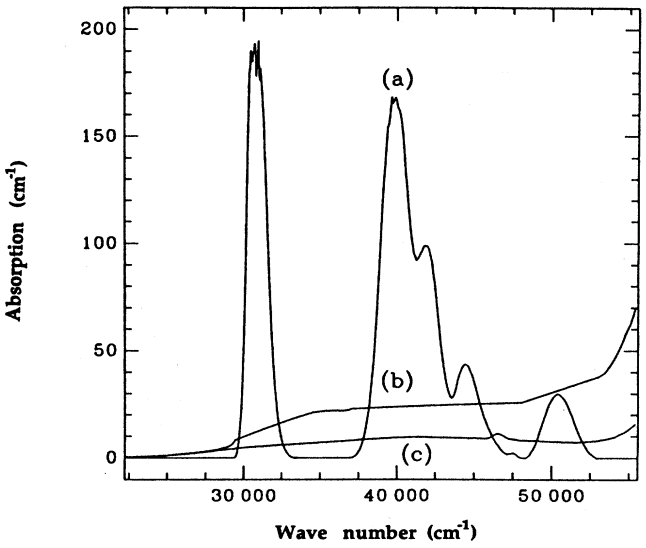

FIG. 3. (a) Room-temperature absorption spectrum for the nominally 20% Ce^{3+}:$LuPO_4$ crystal with background absorption subtracted. (b) Simulated background absorption. (c) Room-temperature absorption spectrum of $LuPO_4$.

the entire 30 000–50 000-cm^{-1} range. Similar features appear in the absorption spectra of pure $LuPO_4$. However, attempts to remove this background in the Ce^{3+}:$LuPO_4$ spectra by simply subtracting the $LuPO_4$ spectrum did not seem justified due to the observed variations in the background from sample to sample.

The approach utilized in carrying out the data analyses was to pick, for each concentration, a smooth background such that after subtraction the remaining spectra scaled as the known Ce^{3+} concentrations. This method seemed to work fairly well. For example, Fig. 3 shows the corrected spectrum for the nominally 20% Ce^{3+} crystal, the subtracted background, and the spectrum of a pure $LuPO_4$ crystal. The integrated absorptions for the Ce^{3+} peaks for the three different concentrations after background subtraction are listed in Table I. The areas

TABLE I. Room-temperature integrated absorptions, $\int_{\text{peak}}\alpha(k)dk$, for $Ce_xLu_{1-x}PO_4$, where x represents the proportion of Ce^{3+} in the starting materials.

Absorption peak (cm^{-1})	Integrated absorption (10^{-3}) $x=0.01$	$x=0.10$	$x=0.20$
31 000	31.4	120.3	299.9
39 800	40.9	117.5	395.0
42 000	13.3	67.7	150.6
44 500	6.9	28.1	79.7
50 500	3.0	32.5	66.1
sum for all peaks	95.5	366.1	991.3
sum with background	529.7	1215	1682

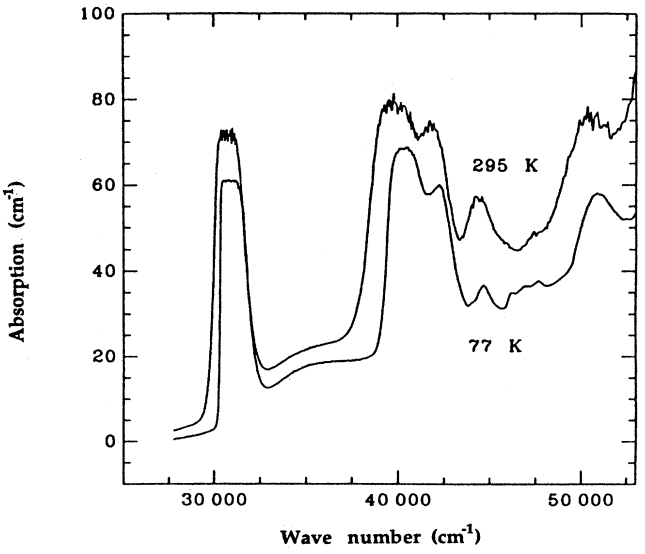

FIG. 4. Room-temperature and 77-K absorption spectra of the nominally 10% Ce^{3+}:$LuPO_4$ crystal.

of the peaks at 31 000 and 50 500 cm^{-1} were obtained by direct integration of the spectra. The peaks at 39 800, 42 000, and 44 500 cm^{-1} overlap significantly, so it was necessary to fit each spectrum in this region with three overlapping asymmetric Gaussian functions. Although there was a certain amount of arbitrariness in these fits, the sums of the areas of the three fitted lines accurately represented the integrated absorptions for this region.

Examination of Table I indicates that, with the selected backgrounds, the integrated absorptions scale fairly accurately. The highest error appears to occur for the peak at 50 500 cm^{-1}. This is not surprising since the largest background absorption is in this region. Table I also includes the sums of the integrated absorptions of the Ce^{3+} peaks after background subtraction and, as an upper limit to this sum, the integrated absorptions from 30 000 to 50 000 cm^{-1} including the background. Oscillator strengths can be calculated easily from these values and are listed in the following section.

Spectra were taken also at 4.2 and 77 K. The absorption spectra of a nominally 10% Ce^{3+}:$LuPO_4$ crystal taken at room temperature and at 77 K are shown in Fig. 4. The differences between the two spectra are not dramatic. There is a shift in the room-temperature spectrum toward lower energies. This is probably due to absorption from thermally populated excited states that are either of vibrational or electronic origin.

B. Calculation of the oscillator strengths

For an ion embedded in a crystal, the oscillator strength associated with a polarized electric dipole transition between an initial state $|i\rangle$ and a final state $|f\rangle$ is given by

$$P_{fi\hat{e}}=\frac{L^2}{n}\frac{4\pi\alpha_{\rm FS}}{r_0}k|\langle f|\hat{e}\cdot\mathbf{D}|i\rangle|^2 , \quad (4)$$

where $\alpha_{\rm FS}=e^2/\hbar c\approx\frac{1}{137.04}$ is the fine-structure (FS) constant, k is the wave number of the light absorbed in the transition, $\hat{e}$ is a unit vector describing the polarization direction of the light, $\mathbf{D}$ is the electric dipole operator, n is the index of refraction of the host crystal, and L is the local-field correction factor. L is related to the index of refraction of the host crystal and is given by the expression[30]

$$L=\frac{n^2+2}{3} . \quad (5)$$

$LuPO_4$ is birefringent, so the value of L is anisotropic. The values of the indices of refraction of $LuPO_4$ are assumed to be equal to the known values for the very similar crystal YPO_4, for which $n_X=n_Y=1.721$ and $n_Z=1.816$ $\lambda=589.3$ nm.[31]

During a $4f\rightarrow 5d$ transition the vibrational state of the crystal also may change as well as the electronic state due to the difference in coupling of the lattice with the $4f$ electron (weak) and with the $5d$ electron (weak to moderate). Thus, in order to accurately describe such an electronic transition, the phonon vibrational state should be included in the initial- and final-state descriptions. If it is assumed that the Born-Oppenheimer approximation holds (although this may not be entirely valid for the $5d$ electron), the wave functions can be written as the product of electronic state of the rare-earth ion and the vibrational state of the crystals, i.e.,

$$|f\rangle=|f_e\rangle\,|\chi^m_{f_e}\rangle , \quad (6)$$

where $|\chi^m_{f_e}\rangle$ represents one particular vibrational mode of the crystal, with the superscript m representing the occupation number of that mode. All vibrational modes may be described in a similar way.

The expression for the oscillator strength is written as

$$P_{fi\hat{e}}=\frac{L^2}{n}\frac{4\pi\alpha_{\rm FS}}{r_0}k|\langle f_e|\hat{e}\cdot\mathbf{D}|i_e\rangle|^2\,|\langle\chi^m_{f_e}|\chi^n_{i_e}\rangle|^2 , \quad (7)$$

where the vibrational part of the wave function has been separated out since it does not depend explicitly on the electronic coordinates of the rare-earth ion. In the absorption measurements discussed earlier, the areas under the observed broad peaks included all the transitions to a particular final electronic state. Equation (7) can be summed over all possible final vibrational states associated with the final electronic state and, in addition, summed over all possible initial electronic states and their associated vibrational states. In the summation over initial states, each term is weighted by a Boltzmann factor. With the assumption that the vibrational properties of the lattice are independent of the rare-earth ion's electronic states for all states of the $4f$ configuration, the summation over the vibrational quantum numbers reduces to unity.[32] The oscillator strength associated with the observed unresolved peaks can be written simply as

$$P_{f\hat{e}}=\frac{L^2}{n}\frac{4\pi\alpha_{FS}}{r_0}k\frac{\sum_p e^{-\beta E_{ip}}|\langle f_e|\hat{e}\cdot\mathbf{D}|i_{ep}\rangle|^2}{\sum_p e^{-\beta E_{ip}}}, \quad (8)$$

independent of the details of the vibrational wave functions. This remains true when all the vibrational modes are explicitly considered.

The expression for summed oscillator strengths depends solely on the dipole matrix elements between wave functions describing the electronic state of the rare-earth ion. These matrix elements are most easily evaluated by expressing the operator $\hat{e}\cdot\mathbf{D}$ as linear combinations of the spherical electric dipole operators,[6] D_q^1. The values of the matrix elements for the circularly polarized dipole operators are given by

$$\langle f_e|D_q^1|i_e\rangle=\langle 5d|r|4f\rangle\langle 2\|C^{(1)}\|3\rangle\sum_{J,M_J}\sum_{J'M_J'}a_{i_eJM_J}a^*_{f_eJ'M_J'}(-1)^{J'-M_J}\begin{bmatrix}J' & 1 & J\\ -M_J' & q & M_J\end{bmatrix}$$
$$\times(-1)^{L'+S'+J+1}(2J+1)^{1/2}(2J'+1)^{1/2}\begin{Bmatrix}J' & 1 & J\\ L & S & L'\end{Bmatrix}\langle L'\|U^1\|L\rangle . \quad (9)$$

The reduced matrix element of the spherical tensor operator, $\mathbf{U}^1$, is unity for a one-electron system. The value of the radial integral, $\langle 4f|r|5d\rangle$, is known from the Hartree-Fock calculations to be 0.441 Å for Ce^{3+}. The value of $\langle l'=2\|C^2\|l=3\rangle$ is 1.73. No polarizers were used in the experimental measurements, so that for comparison purposes the calculated oscillator strengths are averaged over all polarizations. The light was incident along the crystal $\hat{Y}$ axis,[23] and thus the measured oscillator strengths correspond to averages of the oscillator strengths calculated for the $\hat{X}$- and $\hat{Z}$-polarized electric dipole operators. Finally, all the electronic states are actually Kramers doublets, so the final oscillator strengths are averaged over the oscillator strengths for the doublets of the initial states and summed over the oscillator strengths for the doublets of the final states.

C. Comparison of the measured and calculated oscillator strengths and discussion

The results of the oscillator-strength calculations are compared in Table II to the measured oscillator strengths for the nominally 20% Ce^{3+}:$LuPO_4$ crystal at both room temperature and ~10 K. There is little difference between the results for the two temperatures. The observed total $4f\rightarrow 5d$ oscillator strength is about 5 times smaller than the corresponding calculated value. The largest discrepancy between the calculated and measured values occurs for the transition to the highest-energy level of the $5d$ configuration, while the smallest discrepancy occurs for the transition to the lowest-energy level.

The small experimental oscillator strengths are in accord with what has been observed for Ce^{3+} in aqueous solution. For that case, the $4f\rightarrow 5d$ oscillator strength[20] of 0.022 was approximately 2 times smaller than the value of 0.047 calculated by Judd using a partial sum rule for oscillator strengths,[19]

$$\sum_b P_{ab}=\frac{2N}{7}\frac{L^2}{n}\frac{\Delta E}{E_0}\left\langle 4f\left|\frac{r}{a_0}\right|5d\right\rangle^2, \quad (10)$$

where a represents a state of the $4f^N$ configuration and b labels the states of the $4f^{N-1}5d$ configuration. ΔE is the energy difference (in cm^{-1}) between a and b (assumed to be constant for all b), $E_0=219\,475$ cm^{-1}, and $a_0=0.5292$ Å. Evaluating Eq. (10) for Ce^{3+} in $LuPO_4$ yields a value for that $4f\rightarrow 5d$ oscillator strength of 0.055, which is in good agreement with the value of approximately 0.059 calculated in this paper.

A review of the literature shows that the $4f\rightarrow 5d$ oscillator strengths for Ce^{3+} in solid-state systems are, in general, smaller than the values calculated using the Judd sum rule. A comparison of calculated and observed oscillator strengths for Ce^{3+} in various crystals is shown in Table III along with the values of the quantities used in evaluation of Eq. (10). The observed oscillator strengths were derived from various published spectra. This approach is, at best, very approximate. The values of the

TABLE II. Observed and calculated oscillator strengths for the nominally 20% Ce^{3+}:$LuPO_4$ crystal at temperatures of 10 and 295 K.

	$T=10$ K			$T=295$ K		
Peak	10^2P		Ratio	10^2P		Ratio
(cm^{-1})	Calculated	Observed	calc./obs.	Calculated	Observed	calc/obs.
30 468	0.88	0.35	2.5	0.86	0.37	2.3
39 391	1.05	0.36	2.9	2.21	0.49	4.5
41 626	0.81	0.20	4.1	0.63	0.19	3.3
44 038	0.40	0.05	8.0	0.44	0.10	4.4
50 290	2.7	0.14	19	1.98	0.08	25
Total	5.8	1.1	5.3	6.12	1.23	5.0

TABLE III. Comparison between calculated and observed $4f \rightarrow 5d$ oscillator strengths for Ce^{3+} in various host crystals. *M-L* is the average metal ion-ligand distance. $\overline{\Delta E}$ is the average $5d^1$ energy. *n* is the refractive index used in Eq. (10). The observed oscillator strengths for YAG and YLF are lower limits because the actual Ce^{3+} concentration could be substantially lower than the nominal amount in the starting materials (see text).

Host crystal	Coordination	*M-L* (Å)	$\overline{\Delta E}$ (cm^{-1})	Lowest 5*d* (cm^{-1})	*n*	$10^2 P_{cal}$	$10^2 P_{obs}$
$LuPO_4$	8	2.309[a]	41 570	30 700	1.75[b]	5.5[c]	1.24[d]
YAG[e]	8	2.368[f]	34 200	22 040	1.9[g]	5.7	0.57[h]
aquo	9	2.575[i]	44 000	39 000	1.3[j]	4.7	2.2[k]
$YAlO_3$	9	2.62[k]	37 940	39 920	2[l]	6.9	4.0[m]
YLF	8	2.269[n]	43 690	34 270	1.5[o]	5.3	0.48[p]
CaF_2	8	2.364[q]	44 500	32 400	1.434[r]	5.1	1.7[s]
SrF_2	8	2.511[q]	45 730	33 600	1.442[r]	5.3	2.5[s]
LaF_3	9	2.52[t]	44 380	40 600	1.6[u]	5.8	2.1[v]
BaF_2	8	2.685[q]	45 940	34 200	1.475[r]	5.5	4.4[s]

[a]Reference 26.
[b]Reference 31.
[c]Calculated using Eq. (11).
[d]This work.
[e]Only four of an expected five $5d^1$ levels were observed due to the transmission cutoff of the YAG crystal.
[f]Reference 35.
[g]Reference 36.
[h]Reference 37.
[i]Reference 38.
[j]Reference 31.
[k]Reference 39.
[l]Reference 40.
[m]Reference 41.
[n]Reference 42.
[o]Reference 43.
[p]Reference 44.
[q]Reference 45.
[r]Reference 46.
[s]Reference 31.
[t]Reference 47.
[u]Reference 48.
[v]Reference 49.

quantities that might be useful in attempts to explain the variations in $4f \rightarrow 5d$ oscillator strengths are also listed in Table III. The average Ce^{3+}-ligand distance is most obviously correlated to the oscillator strengths. The values given in the table are actually averages over the metal-ion—neighboring-ligand distances for the pure crystal. In general, the smaller this distance, the greater the reduction of the $4f \rightarrow 5d$ oscillator strength relative to the expected free-ion value. This is true whether the surrounding ligands are oxygen or fluorine ions.

The correlation could reflect only the different solubilities of Ce^{3+} in the various crystal hosts. In many of the earlier studies the exact concentrations of Ce^{3+} were not of crucial importance, so that only starting material concentrations were reported. We have shown that the actual concentration of Ce^{3+} in a crystal can be substantially smaller than the concentration in the starting materials. An assumed value for the Ce^{3+} concentration in Eq. (3) that is too large will lead to reduced values for the oscillator strengths determined from the absorption spectra. Thus, the above correlation will follow directly if the solubility of Ce^{3+} in a crystal is related to the metal-ion–ligand distance. Such a relationship might be expected for cases in which the host metal ion is smaller than the cerium ion (i.e., Y^{3+} and Lu^{3+}). Such a relationship does not follow as readily for the crystals CaF_2, SrF_2, BaF_2, and LaF_3, however, since in these cases the metal ion is the same size or larger than Ce^{3+}. In addition, the Ce^{3+} concentrations for $LuPO_4$ and $YAlO_3$ are known from analyses. Thus, for a majority of the crystals, the correlation can not be explained by errors in the Ce^{3+} concentration.

A possible explanation for the correlation can be based on the neuphelauxetic effect.[33] It is generally accepted that, upon introduction of a rare-earth ion into a solid-state system, the rare-earth-ion orbitals expand radially as a result of overlap with the ligand orbitals. This interaction of the ligand and rare-earth-ion orbitals may be viewed as a first step toward covalent bonding. The effect is expected to be much greater for the 5*d* orbitals than for the shielded 4*f* orbitals. Krupke[34] has noted that a differential expansion of the 5*d* orbitals relative to the 4*f*

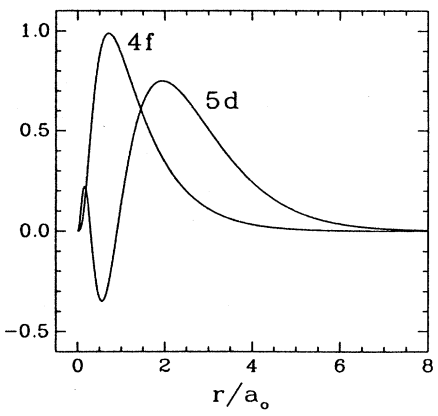

FIG. 5. Hartree-Fock calculated radial wave functions for the 4*f* and 5*d* orbitals of Ce^{3+}.

orbitals could lead to a substantially reduced dipole matrix element $\langle 4f|r|5d\rangle$. This possibility becomes evident when one notes that $|4f\rangle$ and $|5d\rangle$ wave functions have opposite signs in some regions of space as shown in Fig. 5. The correlation of reduced $4f \rightarrow 5d$ oscillator strength with decreases in the Ce^{3+}-ligand distance can thus be seen as a consequence of the greater expansion of the $5d$ wave function as the $5d$-orbital–ligand-orbital overlap increases.

IV. $4f \rightarrow 4f$ ELECTRONIC RAMAN SCATTERING

A. Measurement of the absolute cross sections

The differential scattering cross section per unit solid angle per ion is defined by the relation

$$N_s = n_0 l N_0 \frac{d\sigma}{d\Omega} , \tag{11}$$

where N_s is the number of photons scattered per unit time per unit solid angle, N_0 is the number of photons incident on the sample per unit time, l is the sample thickness, and n_0 is the number density of ions. This expression is valid in cases in which the scattering does not severely deplete the incident beam $[n_0 l (d\sigma/d\Omega) \ll 1]$.

If the value of N_s is known for a given transition, the differential scattering cross section for the transition can be determined directly from Eq. (11). Absolute values of N_s cannot be measured directly from the scattering spectra, however, since the efficiency of the experimental light-collection system is unknown. All that can be determined directly from the spectra are the relative values of the differential scattering cross sections between different transitions.

In order to overcome this difficulty, the scattering from a crystal of $LuPO_4$ (specifically, the $\hat{X}\hat{Z}$ 1034-cm^{-1} vibrational transition) was compared to the scattering from a sample with a known scattering cross section, the 992-cm^{-1} vibrational Raman transition in benzene. The 992-cm^{-1} transition in benzene has a differential scattering cross section of 2.57×10^{-29} cm^2 per steradian of solid angle.[50] The benzene sample was contained in a quartz cuvette with the side facing the collection lens masked in order to approximate the shape and size of the $LuPO_4$ crystals. If S_c and S_b are the scattering signals measured from $LuPO_4$ and benzene, respectively, then the differential scattering cross section for the $\hat{X}\hat{Z}$ 1034-cm^{-1} transition in $LuPO_4$ is given by

$$\left[\frac{d\sigma}{d\Omega}\right]_c = \frac{S_c n_{0b} l_b}{S_b n_{0c} l_c} \frac{\varepsilon_b}{\varepsilon_c} \left[\frac{d\sigma}{d\Omega}\right]_b , \tag{12}$$

where all quantities are defined as in Eq. (11). The factor $\varepsilon_b/\varepsilon_c$ is a correction term to account for the differences of the indices of refraction between $LuPO_4$ and benzene. Benzene has an index of refraction of approximately 1.5 (Ref. 31) [and is contained in a quartz cuvette with an index of refraction of approximately 1.55 (Ref. 31)] while $LuPO_4$ has a refractive index of approximately 1.75. Thus reflection losses are larger and the solid angle of collection is smaller for $LuPO_4$ relative to the benzene sample. The correction factor is calculated to be approximately 1.4 for a collection lens with an f number of 1.2. The differential scattering cross section for the $\hat{X}\hat{Z}$ 1034-cm^{-1} transition of $LuPO_4$ is found to be 1.28×10^{-30} $cm^2\,sr^{-1}$ from the measurements of the two samples and the correction factor.

In our earlier work on electronic Raman scattering in Ce^{3+}:$LuPO_4$, all the scattering intensities were scaled relative to the $\hat{X}\hat{Z}$ 1034-cm^{-1} Raman transition.[23] Thus, the absolute electronic Raman differential scattering cross sections can be determined from these earlier results, the value for the absolute differential scattering cross section for the $\hat{X}\hat{Z}$ 1034-cm^{-1} Raman transition, and the actual Ce^{3+}:$LuPO_4$ concentration. The resulting differential scattering cross sections are listed in Table IV. It is estimated that these values are accurate to within a factor of 2.

B. Calculation of the absolute cross sections

The differential scattering cross section for a Raman transition from an initial state $|i\rangle$ to a final state $|f\rangle$ is given by[51]

$$\frac{d\sigma}{d\Omega} = (2\pi\alpha_{FS})^2 \Lambda k k_s^3 \times \left| \sum_r \frac{\langle f|\hat{e}_s\cdot\mathbf{D}|r\rangle\langle r|\hat{e}\cdot\mathbf{D}|i\rangle}{k_{ri}-k} + \frac{[\hat{e}_s \leftrightarrow \hat{e}]}{k_{rf}+k_s} \right|^2 , \tag{13}$$

where $\hat{e}$ and $\hat{e}_s$ describe the polarizations of the incident and scattered light, respectively, hck and kck_s are the energies of the incident and scattered photons, respectively,

TABLE IV. Measured differential scattering cross sections for electronic Raman scattering in $Ce^{3+}LuPO_4$.

Transition Δ (cm^{-1})	$10^{30}(d\sigma/d\Omega)$ (cm^2/sr) $\hat{X}\hat{Y}$	$\hat{Z}\hat{Z}$	$\hat{X}\hat{Z}$	$\hat{Z}\hat{Y}$	All polarizations
240	0.6	0	0	0	0.3
429	1.6	1.2	9.5	2.5	7.4
2179	0.5	1.8	1.1	3.1	3.25
2221	1.7	0	1.9	0.2	1.9
2620	0.7	0	1.8	0.2	1.35
2676	0.6	0	0.5	0	0.55

and hck_{ri} is the energy difference between the states $|r\rangle$ and $|i\rangle$. The term Λ accounts for the refractive index of the host crystal. Following Dexter,[30] an expression for Λ may be derived and is given by

$$\Lambda=\frac{n_{\hat{e}_s}}{n_{\hat{e}}}L^2_{\hat{e}}L^2_{\hat{e}_s}\ , \tag{14}$$

where n is the index of refraction, and L is the field-correction factor given in Eq. (5).

The states $|r\rangle$ are the virtual intermediate states of the Raman process. In order for the electric dipole matrix elements to be nonzero, the states $|r\rangle$ must have parity opposite that of the states $|i\rangle$ and $|f\rangle$. For electronic Raman scattering from rare-earth crystals, the initial and final states are both associated with the rare-earth-ion $4f^N$ electronic configuration, so that the opposite-parity states closest in energy are from the $4f^{N-1}5d$ configuration. As a first approximation, one assumes these states to be the dominant virtual intermediate states in the electronic Raman process. This assumption directly connects the electronic Raman scattering differential cross sections and the $4f\rightarrow 5d$ oscillator strengths.

In our earlier work on electronic Raman scattering in Ce^{3+}:$LuPO_4$, the relative electronic Raman scattering intensities between different transitions were computed in two ways. The first method followed Axe's standard calculation for two-photon processes in rare-earth ions.[6] This approach assumed that average values may be given to the denominators in Eq. (13) for all the states in a given configuration as in the Judd-Ofelt one-photon calculation.[1,2] Closure was then performed over the states of each configuration separately. The result was an expression containing matrix elements of the spherical unit tensors $\mathbf{U}^1$ and $\mathbf{U}^2$, between the angular parts of the initial- and final-state wave functions and two associated radial parameters, F_1 and F_2. These radial parameters are defined as

$$F_t(k)=(-1)^t\sum_{4f^{N-1}n'l'}\left[\frac{1}{\bar{k}_{n'l'}-k}+\frac{(-1)^t}{\bar{k}_{n'l'}+k}\right]\langle 4f\|C^{(1)}\|l'\rangle^2\langle 4f|r|n'l'\rangle^2(2t+1)^{1/2}\begin{Bmatrix}1&3&l'\\3&1&t\end{Bmatrix}, \tag{15}$$

where the sum is over all excited-state configurations of the form $4f^{n-1}n'l'$, with parity opposite that of the ground-state configuration. Hartree-Fock radial wave functions are used to explicitly evaluate F_1 and F_2 so that the absolute differential scattering cross sections can be obtained. Assuming a contribution only from the $5d^1$ configuration and using a value of $\bar{k}_{5d}=40\,000\ \mathrm{cm}^{-1}$ along with the angular terms evaluated previously,[23] the differential scattering cross sections have been calculated.

The second calculation employed in the earlier work was an evaluation of the sum over intermediate states using the angular parts of the $4f^1$ and $5d^1$ wave functions obtained from crystal-field fits. The absolute differential scattering cross sections are obtained by simply scaling these results by $|\langle 4f|r|5d\rangle|^4|\langle 2\|C^{(1)}\|3\rangle|^4$.

C. Comparison between the measured and calculated cross sections

A comparison between the observed and calculated differential scattering cross sections is given in Table V. In this table the cross sections have been averaged over polarizations and summed over the crystal-field levels of each Russell-Saunders multiplet. The comparison shows that the observed differential cross sections are smaller than both sets of calculated values. The calculation using the closure approximation, however, yields values closer to the observed values than the calculation in which the $5d^1$ wave functions and energies are explicitly used. This is surprising in that it has been shown[23] that the explicit calculation predicts the relative electronic Raman differential scattering cross sections much more accurately.

To rationalize these results, one has to look at the previous discussion of $4f\rightarrow 5d$ oscillator strengths. The $4f\rightarrow 5d$ oscillator strengths for Ce^{3+} in $LuPO_4$ are, on the average 5.3 times smaller than calculated. For the lowest-energy $5d$ level, the observed oscillator strength is 2.5 times smaller than the calculated value. We have suggested that this reduction results from a decrease in the value of the radial integral $\langle 4f|r|5d\rangle$ in the solid state relative to the free or gaseous state. It follows that the electronic Raman differential scattering cross sections should be reduced by factors on the order of $(2.5)^2\approx 6.3$ to $(5.3)^2\approx 30$. It can be seen from Table V that the results of the explicit calculation fall into this range.

TABLE V. Observed and calculated electronic Raman differential scattering cross sections for Ce^{3+} in $LuPO_4$. The transition $^2F_{5/2}\rightarrow{}^2F_{5/2}$ includes transitions from the ground state to the levels at 240 and 429 cm^{-1}. The transition $^2F_{5/2}\rightarrow{}^2F_{7/2}$ includes transitions from the ground state to the levels at 2179, 2221, 2620, and 2676 cm^{-1}.

	$10^{30}(d\sigma/d\Omega)$ (cm^2/sr)			
Transition	Observed	Calculated Judd-Ofelt	Calculated $5d$ wave functions	Calculated weighted $5d$ wave functions
$^2F_{5/2}\rightarrow{}^2F_{5/2}$	7.7	76.8	105	10.6
$^2F_{5/2}\rightarrow{}^2F_{7/2}$	7.1	9.0	35.5	7.2

A more detailed calculation may be performed if an assumption is made regarding the nature of the reduction in the radial integral $\langle 4f|r|5d\rangle$. The measured oscillator strengths are smaller than their respective calculated values by factors ranging from 2.5 to 19. In the above estimate we used the reduction factor for the lowest $5d^1$ level and the average reduction factor for the entire $5d^1$ configuration to calculate the expected reduction of the electronic Raman scattering cross sections. A more accurate description would include all the reduction factors. Accordingly, a calculation has been made in which each term in the summation over the $5d^1$ states in Eq. (13) is weighted by a factor given by the square root of the ratio of the measured oscillator strength to the calculated oscillator strength for that particular $5d^1$ state. The differential scattering cross sections are then given by

$$\frac{d\sigma}{d\Omega}=(2\pi\alpha_{\rm FS})^2\Lambda k k_s^3\left|\sum_r \zeta_r A_{ifr}\right|^2, \tag{16}$$

where

$$A_{ifr}=\frac{\langle f|\hat{\mathbf{e}}_s\cdot\mathbf{D}|r\rangle\langle r|\hat{\mathbf{e}}\cdot\mathbf{D}|i\rangle}{k_{ri}-k}+\frac{[\hat{\mathbf{e}}_s\leftrightarrow\hat{\mathbf{e}}]}{k_{rf}+k_s} \tag{17}$$

and

$$\zeta_r=\left[\frac{(\text{measured oscillator strength})_r}{(\text{calculated oscillator strength})_r}\right]^{1/2}. \tag{18}$$

This calculation is justified as long as the reduction factor associated with a given $4f\rightarrow 5d$ transition ζ_r is independent of the particular $4f$ state under consideration. In other words, we have assumed that the reduction in the radial overlap integral results solely from the expansion of the $5d$ orbitals and that the $4f$ orbitals retain their free-ion radial distributions.

The results of the weighted calculation are compared to the measured cross sections in Tables V and VI and the earlier results of the explicit calculation without weighting. The comparison is surprising in the degree to which the weighted calculation agrees with the measured values of the differential scattering cross sections. This agreement may be somewhat fortuitous given the large uncertainty in the measurement of the cross sections (a factor of 2). Even given this error, however, the results of the calculation with weighting are impressive. In addition, examination of Tables V and VI shows that the calculation with weighting offers a slight improvement over the calculation without weighting in describing the relative values of the cross sections for the different transitions.

The above discussion is based on the assumption that the states of the $5d^1$ electronic configuration serve as the primary intermediate channels in the electronic Raman scattering process. The results of the present work seem to indicate that this is the case for Ce^{3+} in $LuPO_4$. This may not, however, be the case in general. The results of several one- and two-photon intensity experiments in rare-earth solids are most readily explained by the inclusion of g-orbital effects.[14,34,52,53] If all the g orbitals are considered to be degenerate in energy, it can be shown[1] by closure that their contribution to the electronic Raman scattering process is proportional to $|\langle 4f|r^2|4f\rangle|^2$. As pointed out most recently by Chase and Payne[22] and earlier by Krupke,[34] this radial integral does not vary significantly with the radial expansion of the rare-earth-ion orbitals. In addition, in the solid state the energy of the g-type orbitals may be substantially reduced from the free-ion values. Thus, one can imagine situations in which these orbitals contribute significantly to the electronic Raman scattering process. In such cases, the $4f\rightarrow 5d$ oscillator strengths could be much smaller than expected, with electronic Raman cross sections not being proportionally reduced.

V. CONCLUSIONS

For Ce^{3+} in $LuPO_4$ the intensities of the two parity-allowed optical processes, $4f\rightarrow 5d$ absorption and $4f\rightarrow 4f$ electronic Raman scattering, are both smaller than expected from calculations based on free-ion estimates of the radial wave functions. These results can be explained in terms of a reduction of the radial integral $\langle 4f|r|5d\rangle$ in the solid state. Furthermore, a compilation of data on $4f\rightarrow 5d$ oscillator strengths for Ce^{3+} in other crystals hosts indicates that a reduction in the value of this radial integral is correlated with the Ce^{3+}-ligand distance. The nearer the ligands are to the cerium ion, the greater the reduction. It is suggested that a reduction in the value of $\langle 4f|r|5d\rangle$ does not always result in a corresponding reduction in the electronic Raman cross section, however, if contributions from intermediate states

TABLE VI. Observed and calculated electronic Raman differential scattering cross sections for Ce^{3+} in $LuPO_4$.

	$10^{30}(d\sigma/d\Omega)$ (cm/sr)		
Transition Δ (cm^{-1})	Observed	Calculated $5d$ wave functions	Calculated weighted $5d$ wave functions
240	0.3	31	2.8
429	7.4	74	7.8
2179	3.25	20	2.9
2221	1.9	5.3	1.9
2620	1.35	6.7	1.9
2676	0.55	3.5	0.5

other than those associated with the $4f^{N-1}5d^1$ configurations are significant.

ACKNOWLEDGMENTS

We would like to thank B. R. Judd for initially pointing out to us the discrepancies between observed and calculated $f \rightarrow d$ oscillator strengths and for supplying us with a copy of Ref. 19 prior to publication. Thanks also go to Xia Shangda and J. A. Koningstein for helpful suggestions and for a critical review of the manuscript. Finally, we would like to thank Robert Giauque and Linda Sindelar for performing the x-ray-fluorescence analysis. This research was supported in part by the Director, Office of Energy Research, Office of Basic Energy Science, Chemical Sciences Division, the U. S. Department of Energy, under Contract No. DE-AC03-76SF00098. Oak Ridge National Laboratory is operated by Martin Marietta Energy Systems, Inc for the U. S. Department of Energy, under Contract No. DE-AC05-84OR21400.

*Present address: Naval Research Laboratory, Washington, D.C. 20375-5000.

[1]B. R. Judd, Phys. Rev. **127**, 750 (1962).

[2]G. S. Ofelt, J. Chem. Phys. **37**, 511 (1962).

[3]C. K. Jørgensen and B. R. Judd, Mol. Phys. **8**, 281 (1964).

[4]S. F. Mason and R. D. Peacock, Mol. Phys. **30**, 1829 (1975).

[5]R. D. Peacock, Struct. Bonding (Berlin) **22**, 88 (1975).

[6]J. D. Axe, Phys. Rev. **136**, A42 (1964).

[7]M. Dagenais, M. Downer, R. Neumann, and N. Bloembergen, Phys. Rev. Lett. **46**, 561 (1981).

[8]M. C. Downer, A. Bivas, and N. Bloembergen, Opt. Commun. **41**, 355 (1982).

[9]M. C. Downer and A. Bivas, Phys. Rev. B **28**, 3677 (1983).

[10]Michael Coffin Downer, Ph.D. thesis, Harvard University, 1983.

[11]P. C. Becker, N. Edelstein, G. M. Williams, J. J. Bucher, R. E. Russo, J. A. Koningstein, L. A. Boatner, and M. M. Abraham, Phys. Rev. B **31**, 8102 (1985).

[12]Philippe C. Becker, Ph.D. thesis, University of California, Berkeley, 1986.

[13]B. R. Judd and D. R. Pooler, J. Phys. C **15**, 591 (1982).

[14]P. C. Becker, N. Edelstein, B. R. Judd, R. C. Leavitt, and G. M. S. Lister, J. Phys. C **18**, L1063 (1985).

[15]J. Sztucki and W. Stręk, Phys. Rev. B **34**, 3120 (1986).

[16]J. Sztucki and W. Stręk, Chem. Phys. Lett. **125**, 520 (1986).

[17]J. Sztucki and W. Stręk, Chem. Phys. Lett. **138**, 410 (1987).

[18]M. F. Reid and F. S. Richardson, Phys. Rev. B **29**, 2830 (1984).

[19]B. R. Judd, Inorg. Chim. Acta **139**, 341 (1987).

[20]W. T. Carnall, *Handbook on the Physics and Chemistry of Rare Earth Ions in Solution* (North-Holland, Amsterdam, 1979).

[21]J. V. Beitz, W. T. Carnall, and H. Crosswhite, J. Chem. Phys. **80**, 2301 (1984).

[22]L. L. Chase and S. A. Payne, Phys. Rev. B **34**, 8883 (1986).

[23]G. M. Williams, P. C. Becker, N. Edelstein, J. G. Conway, L. A. Boatner, and M. M. Abraham, preceding paper, Phys. Rev. B **40**, 4132 (1989).

[24]R. D. Cowan, *The Theory of Atomic Structure and Spectra* (University of California Press, Berkeley, 1981).

[25]R. D. Giauque, R. B. Garrett, and L. Y. Goda, Anal. Chem. **49**, 1012 (1977).

[26]W. O. Milligan, D. F. Mullica, G. W. Beall, and L. A. Boatner, Inorg. Chim. Acta **60**, 39 (1982).

[27]F. A. Cottom and G. Wilkinson, *Advanced Inorganic Chemistry*, 5th ed. (Wiley, New York, 1988).

[28]E. Nakazawa and F. Shiga, J. Lumin. **15**, 255 (1977).

[29]Charge-transfer bands for Ce^{3+} should occur at energies considerably higher than those observed for Yb^{3+} in the same crystal host. In Yb^{3+}:$LuPO_4$ the onset of the first charge transfer band has been observed at approximately 48 500 cm^{-1} (see Glen M. Williams, Ph.D. thesis, University of California , Berkeley, 1988).

[30]D. L. Dexter, in *Solid State Physics No. 6, Advances in Research and Application,* edited by F. Seitz and Turnbull (Academic, New York, 1958).

[31]R, C. Weast, *CRC Handbook of Physics and Chemistry,* 59th ed. (Chemical Rubber Co., West Palm Beach, FL, 1978-1979).

[32]C. J. Ballhausen, *Molecular Electronic Structures of Transition Metal Complexes* (McGraw-Hill, London, 1979).

[33]R. Reisfeld and C. K. Jørgensen, *Lasers and Excited States of Rare Earths, Inorganic Chemistry Concepts Vol. 1* (Springer-Verlag, Berlin, 1977).

[34]W. F. Krupke, Phys. Rev. **145**, 325 (1966).

[35]R. W. G. Wyckoff, *Crystal Structures* (Wiley, New York, 1965), Vol. 3.

[36]T. S. Lomheim and L. G. Deshazer, Phys. Rev. B **20**, 4343 (1979).

[37]W. J. Miniscalco, J. M. Pellegrino, and W. M. Yen, J. Appl. Phys. **49**, 6109 (1978).

[38]K. Okada, Y. Kaizu, H. Kobayashi, K. Tanaka, and F. Marumo, Mol. Phys. **54**, 1293 (1985).

[39]S. Geller and E. A. Wood, Acta Crystallogr. **9**, 563 (1956).

[40]M. J. Weber, B. H. Matsinger, V. L. Donlan, and G. T. Stuart, J. Chem. Phys. **57**, 562 (1972).

[41]M. J. Weber, J. Appl. Phys. **44**, 3205 (1973).

[42]P. Blanchfield and G. A. Saunders, J. Phys. C **12**, 4673 (1979).

[43]D. E. Castleberry and A. Linz, Appl. Opt. **14**, 2506 (1975).

[44]D. J. Ehrlich, P. F. Moulton, and R. M. Osgood, Jr., Opt. Lett. **4**, 184 (1979).

[45]R. W. G. Wyckoff, *Crystal Structures* (Wiley, New York, 1965), Vol. 1.

[46]E. Loh, Phys. Rev. **154**, 270 (1967).

[47]A. Zalkin and D. H. Templeton, Acta Crystallogr. Sect. B **41**, 91 (1985).

[48]M. P. Wirich, Appl. Opt. **5**, 1966 (1966).

[49]D. J. Ehrlich, P. F. Moulton, and R. M. Osgood, Jr., Opt. Lett. **5**, 339 (1980).

[50]A. Yariv, *Quantum Electronics* (Wiley, New York, 1975).

[51]R. Loudon, *The Quantum Theory of Light* (Clarendon, Oxford, 1983).

[52]P. J. Becker, Phys. Status Solidi B **43**, 583 (1971).

[53]M. Hasunama, K. Okada, and Y. Kato, Bull. Chem. Soc. Jpn. **57**, 3036 (1974).